

# Juxtacellular recording and morphological identification of single neurons in freely moving rats

Qiusong Tang<sup>1</sup>, Michael Brecht<sup>1</sup> & Andrea Buralossio<sup>1,2</sup>

<sup>1</sup>Bernstein Center for Computational Neuroscience, Humboldt University, Berlin, Germany. <sup>2</sup>Present address: Werner Reichardt Centre for Integrative Neuroscience, Tübingen, Germany. Correspondence should be addressed to M.B. ([michael.brecht@bccn-berlin.de](mailto:michael.brecht@bccn-berlin.de)) or A.B. ([andrea.buralossio@cin.uni-tuebingen.de](mailto:andrea.buralossio@cin.uni-tuebingen.de)).

Published online 11 September 2014; doi:10.1038/nprot.2014.161

**It is well established that neural circuits consist of a great diversity of cell types, but very little is known about how neuronal diversity contributes to cognition and behavior. One approach to addressing this problem is to directly link cellular diversity to neuronal activity recorded *in vivo* in behaving animals. Here we describe the technical procedures for obtaining juxtacellular recordings from single neurons in trained rats engaged in exploratory behavior. The recorded neurons can be labeled to allow subsequent anatomical identification. In its current format, the protocol can be used for resolving the cellular identity of spatially modulated neurons (i.e., head-direction cells and grid cells), which form the basis of the animal's internal representation of space, but this approach can easily be extended to other unrestrained behaviors. The procedures described here, from the beginning of animal training to the histological processing of brain sections, can be completed in ~3–4 weeks.**

## INTRODUCTION

A major goal of contemporary neuroscience is to decipher the logic of neural circuit function and their contribution to behavior. Neural circuits are assembled from a huge variety of neuronal cell types, which differ in morphology, intrinsic properties, molecular identity, microcircuit connectivity and projection patterns<sup>1,2</sup>. Elucidating the cellular basis of behavior therefore requires resolving the contribution of the individual neurons. Work on interneurons has indeed revealed a high degree of morpho-functional cellular specialization and has shown that single-cell resolution is an essential requirement for classifying neurons into distinct classes<sup>3,4</sup>. For principal cells, which make up the large majority of cortical neurons, our knowledge is comparatively limited. Although currently available evidence points to a seemingly complex heterogeneity of functional and structural properties<sup>5–14</sup>, structure-functional relationships at the single-cell level remain to be established.

The quest for the cellular basis of brain function and behavior has been revolutionized by the arrival of optogenetic technologies<sup>15,16</sup>. In combination with electrophysiological<sup>17–19</sup> and optical methods<sup>17,20</sup>, optogenetic approaches make it possible to analyze neural circuits by characterizing cell type-specific functions in behaving animals<sup>21,22</sup>. While providing insights into the structural basis of neural activity and behavior, current optogenetic-based approaches to cell-type identification have two main limitations. The first disadvantage is that they are limited to broadly defined cell groups, identified on the basis of the expression of individual molecular markers or on projection targets<sup>23–25</sup>. Cell types can, however, rarely be identified unequivocally by single features<sup>1,4,26,27</sup>. Second, optogenetic approaches are not ideally suited for resolving the microcircuit structure of cellular activity, as single-cell resolution is required for this. Relating neuronal activity to morphological diversity and microcircuit wiring diagrams is essential for understanding cortical computation and for building biologically realistic models of neural circuit function<sup>28–31</sup>.

Since its establishment<sup>32–34</sup>, the juxtacellular recording and labeling technique has become the method of choice for

investigating structure-function relationships in the nervous system<sup>35</sup>. Owing to methodological limitations, however, most studies have so far focused on simplified (i.e., anesthetized<sup>32–34,36</sup> or awake head-fixed<sup>10,37–39</sup>) preparations. The procedures illustrated in this protocol, consisting of a combination of animal training, electrophysiological recording and juxtacellular labeling procedures<sup>34,40</sup>, enable anatomical visualization of single neurons recorded in freely moving animals, which are engaged in exploratory behavior (Ray *et al.*<sup>8</sup>). The methods described here include two key methodological developments over our previous procedures in Buralossio *et al.*<sup>41</sup> and Herfst *et al.*<sup>42</sup>: recordings are obtained in awake, drug-free animals trained to run in large open-field environments (see ANTICIPATED RESULTS); and ‘head-anchoring’ stabilization procedures<sup>41–43</sup> have been replaced by a removable stabilization seal, which enables multiple penetrations and recording or labeling attempts to be performed in the same animal. We typically label few (one or two) cells in the same animal and brain region, so that the recovered neurons can be unequivocally assigned. Fluorescent dyes for neuronal labeling<sup>44</sup> could potentially be used for increasing the number of recovered neurons. Other neuronal tracers, such as biotinylated dextran amines (i.e., BDA-3000), which are more resistant to intracellular degradation<sup>45</sup>, could be used for improved visualization of long-range axonal projections, as they can be recovered up to a few days after labeling<sup>33,35,46</sup>. The use of low-resistance electrodes, together with close proximity of cell and the recording tip, ensures high signal-to-noise ratios of juxtacellular spike signals<sup>41,42</sup> (see ANTICIPATED RESULTS) and unequivocal spike identification. Recording durations are limited, but depending on the task and the animal's behavioral performance they can nevertheless provide sufficient electrophysiological and behavioral data for functional classification of the recorded neurons (see ANTICIPATED RESULTS).

In summary, this protocol provides complementary information to currently available optical, electrophysiological and genetic-based tools. The method is labor-intensive and of limited output rate (see ANTICIPATED RESULTS); however,

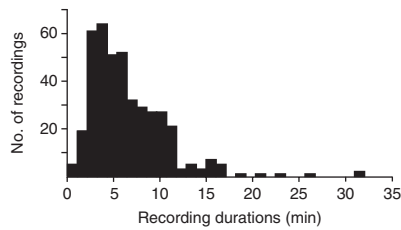


**Figure 1** | Recording durations. Distribution of recording duration for juxtacellular recordings in freely moving animals ( $n = 417$ ). In a large fraction of recordings (74%), a juxtacellular labeling was not attempted (recordings were either lost prematurely, or labeling was deliberately not attempted).

we believe that the ability of this approach for monitoring both behavior and cellular morphology will be very valuable for establishing structure-function relationships in freely behaving animals.

### Experimental design

In this protocol, we describe an optimized procedure for juxtacellular labeling of single neurons recorded from freely behaving animals<sup>8</sup>. Before attempting the full protocol, we suggest that inexperienced experimenters practice the juxtacellular recording and labeling procedure first in anesthetized animals, and then in awake head-fixed animals, until a reliable cell recovery rate (>80%) is achieved. Unequivocal assignment of the recorded neuron(s) is crucial to the protocol; thus, to ensure the specificity of cell labeling, control experiments can be considered, as originally described by Pinault<sup>32,34</sup> and Deschênes *et al.*<sup>33</sup>. For example, experiments in which neurons are (i) recorded in juxtacellular configuration but not stimulated with positive current; (ii) stimulated with negative current; or (iii) stimulated with sub-threshold positive current (i.e., insufficient to induce cell firing) should result in no cell labeling. Killing the recorded neuron by high current injection at the end of the labeling protocol can be used as a proof-of-principle test for the specificity of the juxtacellular labeling procedure (refs. 32,34).

In our current data set from freely moving animals, in ~50% of the cases in which labeling was attempted, a neuron was recovered ( $n = 53$  identified cells out of 111 labeling attempts). Recording durations were up to 32 min, including all recordings ( $n = 417$  from 209 rats; mean  $\pm$  s.d. =  $6.6 \pm 4.1$  min; **Fig. 1**). The recording duration necessarily limits the number of possible experimental questions that can be addressed with this method. As shown in ANTICIPATED RESULTS, the experimental design and animal behavior need to be optimized for obtaining sufficient information within this average time window. It must, however, be noted that the recording durations reported here might be a lower-bound underestimate, as deep recordings in posterior brain structures (such as the parahippocampal cortex—which was the target area in our current data set) are known to be more unstable compared with anterior brain regions<sup>42,47</sup>. Most recording losses occurred upon mechanical disturbances (i.e., head-bumps on the walls or head-shakes). Minimizing the occurrence of such events, together with the stress of the animal by careful habituation to the experimental procedures, has a strong impact in our experience on the recording duration and/or stability.

The techniques and procedures described in this protocol are optimized for rats, but they can be potentially adapted for recording in other animal species. For smaller animals (e.g., mice), further miniaturization of the implant components and/or use of lighter construction materials (e.g., aluminum) should be considered. The applicability of this protocol is, in principle, not restricted by brain area or recording depth, as a ‘clean’ pipette tip is not a necessary requirement for the establishment of juxtacellular recordings; i.e., unlike for whole-cell recordings, electrodes can typically be reused for multiple penetrations and they can be advanced into the brain tissue without positive air pressure. However, application of air pressure might be needed for recording in very deep brain structures (i.e., >4–5 mm from the pial surface) to minimize the likelihood of pipette clogging. In its present formulation, the method focuses on foraging and exploratory behavior, but it can, in principle, be extended to other forms of unrestrained natural or trained behaviors. Different success rates are likely to be expected depending on the target region, cell type and behavior under investigation.

## MATERIALS

### REAGENTS

#### Surgery and electrophysiology

- Experimental animals: Wistar rats (~130–250 g body weight; ~5–9 weeks old).

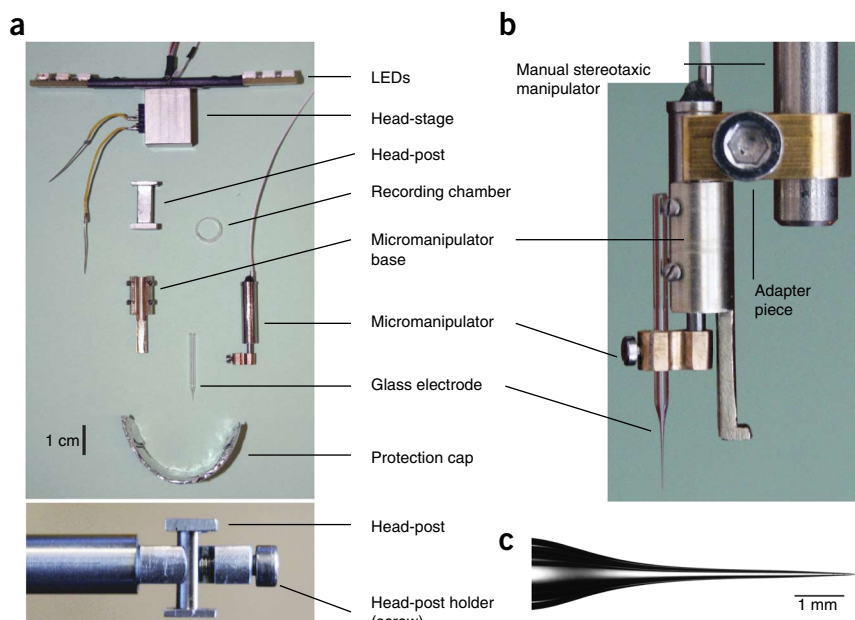
**! CAUTION** Animal experiments must comply with institutional and governmental guidelines. **▲ CRITICAL** As a rule, we do not recommend starting the procedure with rats >300 g of body weight, as the mechanical stress they can exert upon fixation (Step 16) can potentially destabilize the head-implant.

- Isoflurane (Isoflurane CP, CP-Pharma, cat. no. 31303; store it at 4 °C)
- Ketamine (10% (wt/vol), CP-Pharma, cat. no. 400203.00.00; store it at 4 °C)
- Xylazine (2% (wt/vol), Bayer, cat. no. 6293841.00.00; store it at 4 °C)
- Pentobarbital (Narcoren, Merial, cat. no. 6088986.00.00; store it at 4 °C)
- Lidocaine (bela-pharm, cat. no. 6357796.00.00; store it at 4 °C)
- Bupivacaine (Marcaine, Sanofi; store it at 4 °C)
- Analgesic (Rimadyl, Pfizer, cat. no. 400684.00.00; store it at 4 °C)
- UV-curable adhesive (3M ESPE Filtek Silorane, cat. no. 4772TK; store it at 4 °C)
- HEPES (Sigma-Aldrich, cat. no. 54459; store it at room temperature, i.e., 20–25 °C)

- KCl (Sigma-Aldrich, cat. no. 60129; store it at room temperature)
- NaCl (Sigma-Aldrich, cat. no. 71376; store it at room temperature)
- $\text{CaCl}_2$  (Sigma-Aldrich, cat. no. 21108; store it at room temperature)
- $\text{MgCl}_2$  (Sigma-Aldrich, cat. no. 63064; store it at room temperature)
- NaOH solution (Merck KGaA, cat. no. 109137; store it at 4 °C)
- Neurobiotin (VectorLabs, cat. no. SP-1120) **▲ CRITICAL** Store it at –20 °C and protect it from light and moisture. Biotin can be used as an alternative<sup>34</sup>. Biotinylated dextran amines (i.e., BDA-3000) are more resistant to intracellular degradation and they can be used for revealing long-range axonal projections (see INTRODUCTION)
- Agarose (Sigma-Aldrich, cat. no. A9539; store it at room temperature)
- Dental acrylic (Paladur powder and liquid, Heraeus Kulzer; store it at room temperature; mix the two components for preparing dental acrylic according to the manufacturer’s instructions) **! CAUTION** Unpolymerized dental acrylic components can be irritating to the skin and respiratory pathways. Handle it under a fume extractor and follow the producer’s guidelines.
- Instant glue (cyanoacrylate, Henkel, cat. no. 1436519; store it at room temperature)

**Figure 2** | Implant components for obtaining juxtacellular recordings in freely moving animals.

(a) The individual components of the implant that are either cemented (head-post, recording chamber, protection cap and micromanipulator base) or mounted on the rat's head for the recording (head-stage and micromanipulator). The bottom image shows a close-up view of the head-post, secured into the head-post holder by means of a screw. The bottom surface of the head-post is cemented on the animal's head (Step 14), whereas the top surface serves as support for the miniaturized head-stage (Step 26). (b) The assembled micromanipulator-base complex, which is attached to a manual stereotaxic manipulator via an adapter piece. This assembly is used for positioning and implanting the micromanipulator's base (Step 22). (c) High-magnification view of the pipette tip.



- Mitomycin (Sigma-Aldrich, cat. no. M4287; store it at 4 °C)
- Silicone sealant (Kwik-Cast, World Precision Instruments; store it at room temperature)
- Streptavidin conjugated to Alexa Fluor 546 (Life Technologies, cat. no. S-11225; store it at -20 °C)
- Mouse monoclonal anti-calbindin antibody (Sigma-Aldrich, cat. no. C9848; divide it into aliquots and store it at -20 °C)
- Anti-mouse secondary antibodies (i.e., conjugated with Alexa Fluor 488, Life Technologies, cat. no. A-11001; divide it into aliquots and store it at -20 °C)

#### EQUIPMENT

- Faraday cage
- Stereomicroscope (e.g., Olympus, Zeiss)
- Cold light source (e.g., Olympus, Zeiss)
- Stereotaxic apparatus (e.g., Narishige)
- Animal body temperature control system (e.g., FHC)
- Drill system (e.g., Foredom)
- Surgical tools (e.g., Fine Science Tools)
- Surgery absorbent swabs (e.g., SUGI, Kettenbach, cat. no. 31602)
- Blue and red light-emitting diodes (LEDs; e.g., Conrad; red Top-View-LED, cat. no. 175272; blue Top-View-LED, cat. no. 175265)
- Bridge amplifier with miniature head-stage (NPI Electronic, cat. no. ELC-03XS)
- Miniaturized micromanipulator (4 mm diameter, 16 mm length, 9 mm travel distance; Kleindiek Nanotechnik; Fig. 2)
- Audio monitor (e.g., AM10, Grass Technologies)
- Acquisition board (analog-to-digital converter, e.g., Heka LIH 8+8)
- Software for acquiring electrophysiology data (e.g., Patchmaster, Heka; Spike2, CED)
- Animal position tracking system (e.g., Neuralynx)
- Borosilicate glass capillaries (1.5 mm outer diameter, 0.87 mm inner diameter; e.g., Hilgenberg)
- Glass-cutting file (e.g., VWR, cat. no. 470005-474)
- Pipette puller (e.g., P-97, Sutter Instrument)
- Air objective, 100× (e.g., MPLFLN, working distance 1.0 mm, Olympus)
- Hot plate (e.g., VWR, cat. no. 97042-650)
- Microcentrifuge tubes, 0.5 ml (e.g., neoLAB, cat. no. 780500)
- Vibratome (e.g., Microm)
- Cryostat (e.g., Leica)
- UV lamp (e.g., Heraeus) **! CAUTION** Always wear UV-protection glasses upon use.
- UV-light protection glasses (e.g., Heraeus)
- Software and hardware for 3D morphological reconstruction (e.g., Neurolucida, MBF Bioscience)

#### REAGENT SETUP

**Extracellular (Ringer) solution** Extracellular (Ringer) solution is 135 mM NaCl, 5.4 mM KCl, 5 mM HEPES, 1.8 mM CaCl<sub>2</sub> and 1 mM MgCl<sub>2</sub>

(pH is adjusted to 7.2 by adding NaOH; target osmolality is 290 mmol/kg). Make this solution in advance, filter-sterilize it through a 0.2-μm filter and store it at 4 °C for up to several months.

**Pipette solution** Add 1.5–2% (wt/vol) Neurobiotin to the Ringer solution (above). As an alternative, biocytin can also be used. Filter the solution through a 0.2-μm filter, make small aliquots (~5–10 μl) and store them at temperatures ≤ -20 °C. In our experience, aliquots are stable at -20 °C for several months. **▲ CRITICAL** Osmolarity and pH are crucial and should be checked for each batch.

**Agar solution** Add 3% (wt/vol) agarose powder to the Ringer solution and boil it in a microwave. The solution becomes clear. Keep the solution on a hot plate and stir it throughout the experiment so that it can be used as liquid when necessary. The agarose solution can be used after it has cooled down to near physiological temperature. Make the solution in advance before each experiment.

**Ketamine/xylazine** Mix ketamine 10% (wt/vol) with xylazine 2% (wt/vol), resulting in a final concentration of 80 mg/kg ketamine and 6 mg/kg xylazine and injection dose of 0.11 ml/100 g. Supplemental doses should be administered by alternating injections of ketamine and ketamine/xylazine (half of the initial doses) every 30–45 min, or as required. Store the ketamine/xylazine mix at 4 °C for up to 4–6 weeks.

#### EQUIPMENT SETUP

**Recording chamber** Cut off a circular piece (~5 mm diameter and 2 mm height) from the cap of a 0.5-ml microcentrifuge tube (Fig. 2a).

**LED assembly** Mount red and blue LEDs on a linear support (spacing 4.5 cm) and glue them on the miniature head-stage (Fig. 2a). Record the two lights using the video-tracking system (i.e., Neuralynx) and use them *post hoc* for extracting the animal's positional coordinates and heading direction. Alternatively, head-mountable LEDs integrated within the head-stage can also be used (e.g., from NPI Electronic).

**Glass electrodes** Pull pipettes with a long taper, by using a horizontal puller (e.g., P-97, Sutter Instruments). Electrodes should be pulled with a long taper (Fig. 2c), to avoid or minimize brain tissue damage upon electrode penetration, a tip opening of ~1.5–2 μm and a resistance of 4–6 MΩ.

**▲ CRITICAL** The tip of each electrode should be examined at high magnification (>1,000× total magnification, through a 100× air objective; see Equipment). Discard electrodes with irregular, asymmetric shapes.

**Protection cap** The protection cap is plastic, shielded with aluminum foil; Fig. 2a. The protection cap should be light, and it is needed for protecting the implant (in particular the micromanipulator and the recording electrode) during the freely moving behavior. The aluminum foil provides additional electrical isolation from external noise.

**Adaptor piece** The adaptor piece is used for mounting the micromanipulator/base complex on a manual stereotaxic manipulator

## PROTOCOL

**Figure 3** | Assembled implant for juxtacellular recordings in freely moving animals. Schematic diagram showing the position of the individual implant components relative to the rat's head (left, top view; right, side view).

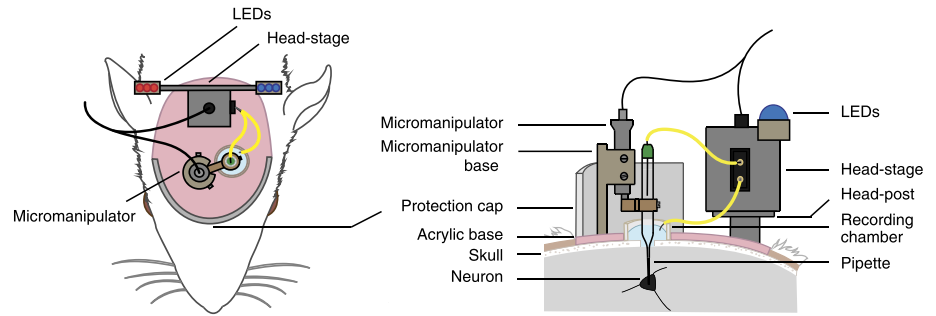


(Fig. 2b; required for implanting the micromanipulator's base on the rodent's head; see Step 22).

**Rat restrainer box** The box is made of polyvinyl chloride (PVC); length  $\times$  width  $\times$  height: 20 cm  $\times$  8 cm  $\times$  8 cm: The restrainer should be equipped with a top lid, as head-fixation in open space is a source of stress and discomfort to the animal<sup>48</sup>.

**Head-post** The head-post is made of aluminum or stainless steel; **Figure 2a**. It is a small piece of metal that is implanted on the rat's head, in tight adherence to the skull, which serves a dual function: to allow head-fixation in the stereotaxic frame and to serve as a base for the miniaturized head-stage (as shown in **Fig. 3**).

**Head-post holder** The head-post holder is made of stainless steel; it is used for holding the head-post and fixing the head of the rat on the

stereotaxic frame. Secure the head-post onto the head-post holder with a screw (**Fig. 2a**).

**Micromanipulator base** The micromanipulator base is made of brass, **Figure 2a**, or aluminum, **Figure 2b**; it is used for mounting the micromanipulator on the rat's head (**Fig. 2**).

**Behavioral arena** A square arena is used in this protocol (1 m  $\times$  1 m). However, different geometrical designs are possible. In particular, elevated platforms (without walls) can be used to diminish the occurrence of recording losses owing to the implant accidentally touching the walls.

## PROCEDURE

### Animal behavioral training ● TIMING 7–10 d

**1** | Progressively familiarize a male Wistar rat (~130–250 g body weight; see MATERIALS) to the experimenter and the restrainer box for at least 3 d. To do this, handle the rat and let it explore the restrainer box in its home cage a few times per day. One or two days before starting the training (Step 2), habituate the rat to chocolate by adding a few crumbs to their regular food pellets.

**! CAUTION** All animal experiments must comply with the relevant institutional and governmental animal care guidelines.

**2** | Train the rat to chase randomly scattered food pellets inside a behavioral arena ('pellet-chasing' foraging task<sup>49</sup>) by placing the animal in the behavioral arena and throwing small chocolate crumbs randomly to initiate and motivate pellet chasing and running. Perform short training sessions (5–10 min) multiple times per day.

**▲ CRITICAL STEP** During training, animals receive unlimited access to food in the experimental arena and a limited food allowance in their cage. Monitor daily the rat's body weight. Under this food regime, animals should consistently maintain >90% of their *ad libitum* body weight; this provides the necessary motivation to the rat to actively engage in the behavioral training.

**▲ CRITICAL STEP** On initial training sessions, animals typically make only short excursions into the environment from their 'home base' location (typically one corner of the arena) by moving along the walls. As training proceeds, this behavior will be slowly replaced by longer excursions eventually crossing the center of the arena. Keep low light conditions in the room, and test animals in their dark phase for optimal behavioral performance. Provide a chocolate reward after each training session in their home cage. Reward the animal with larger chocolate pellets when runs across the center of the arena are made.

**3** | Continue to train the animal until its behavioral performance is satisfactory. For the specifics of our experimental design, this corresponds to continuous running periods of ~20–30 min. This is typically achieved within 3–7 d by multiple (typically up to 4 d) training sessions per day of progressive durations.

**▲ CRITICAL STEP** Behavior is a crucial parameter for the success of the experiment. Daily training sessions at regular times should be performed to maintain the rat at steady-state performance.

### ? TROUBLESHOOTING

**■ PAUSE POINT** Progression to the following steps can be delayed by a few days by keeping the rat at steady-state behavioral performance.

### Implantation and animal recovery ● TIMING 3–6 d

**4** | Anesthetize the animal with an i.p. injection of ketamine/xylazine (80–100 mg/kg ketamine; 10 mg/kg xylazine, see Reagent Setup) according to standard procedures.

**! CAUTION** Appropriate regulations and guidelines for animal experiments must be followed.

**5** | Place the animal on a heating pad and fix the head in the stereotaxic apparatus. Use hair trimmers to shave the scalp above the area of interest.

**6|** Inject a local anesthetic (e.g., lidocaine or bupivacaine) s.c. into the animal's scalp, and gently cover both eyes with ophthalmic cream to prevent drying.

**7|** Use forceps to lift the scalp and scissors to cut and remove a circle of skin. Both the lambda and bregma points on the skull should be made visible. Scrape off connective tissue with a delicate bone scraper by applying gentle pressure.

**▲ CRITICAL STEP** This step and Steps 8–14 should be performed under stereomicroscopic guidance.

**▲ CRITICAL STEP** Minimal bleeding may occur at this point on the skull surface. Clean it thoroughly with Ringer solution, and use cotton/surgery absorbent swabs for drying and cleaning the surface. Proceed to the next step only when bleeding has stopped.

**8|** Rinse the clean skull surface, and let it dry (typically 3–5 min; the bone will appear opaque). Mark your stereotaxic reference point (lambda or bregma) with a permanent marker. It will be used as a reference point for localizing the craniotomy site (Step 19).

**9|** Apply a thin layer of adhesive (e.g., from 3M ESPE; see Reagents) to the nearly dry skull. Cure the adhesive by UV light (follow guidelines from the manufacturer).

**! CAUTION** Protect your eyes from the UV light by means of UV-protection glasses.

**▲ CRITICAL STEP** The glue layer provides a base for the dental acrylic to adhere to. The skull surface should be dry and clean from blood before applying the glue. Traces of blood will prevent glue polymerization and compromise the adherence of the implant to the skull.

**? TROUBLESHOOTING**

**10|** After UV-curing the adhesive, clean the polymerized surface thoroughly with the help of a cotton swab. The polymerized adhesive should appear as a compact, resistant layer.

**? TROUBLESHOOTING**

**11|** Use a stereotaxic atlas<sup>50</sup> to determine the coordinates of the brain region of interest. The marked bregma (or lambda) point is still visible through the thin transparent layer of polymerized adhesive. Mark the position for the center of the craniotomy. Use a permanent marker to mark the location for drilling.

**12|** Glue the recording chamber (see Reagent Setup) onto the exposed skull with adhesive (e.g., from 3M ESPE; see Reagents). Seal the recording chamber edges with solid glue from 3M ESPE to avoid leakage of the dental cement into the chamber (see Step 13 below). Fill the recording chamber with silicone sealant.

**13|** Mix the dental cement and solvent in a weighing dish until it is slightly thickened, and then carefully pour the cement onto the skull and wound margins.

**! CAUTION** Dental cement powder and fumes are irritating and toxic. We recommend this step to be performed under a fume extractor (follow the manufacturer's guidelines for proper use).

**▲ CRITICAL STEP** Avoid allowing the dental cement to enter the recording chamber.

**14|** Allow the cement to harden. Repeat Step 13 for cementing the head-post posteriorly and the shielded protection cap anteriorly (**Fig. 3**).

**15|** Release the rat from the stereotaxic frame and allow the animal to recover on the heating pad. Next, return it to its cage for recovery under observation. Apply postoperative antibiotics and analgesics (e.g., Rimadyl) and follow standard surgical recovery procedures.

**▲ CRITICAL STEP** Animal behavior should be closely monitored to assess recovery; home cage activity, food and water consumption should return to presurgery levels. Allow the rat to fully recover from the surgery (typically 2–5 d) before proceeding to the next step.

### **Habituation to head fixation and training** ● **TIMING 4–6 d**

**16|** Start habituating the animal to the head-fixation by placing the animal in the restrainer box, and by securing the head-post to the head-post holder (**Fig. 2a**, bottom). This first fixation should not last more than 30 s–1 min. The animal is then placed back in its home cage, where a food reward (i.e., chocolate crumbs) is provided for positive reinforcement.

**▲ CRITICAL STEP** Perform the fixation of the head-post to the holder rapidly. On the first session, rats might show overt signs of stress (i.e., vocalization, struggling and defecation). However, these signs will gradually disappear during habituation, and they will typically be virtually absent after 2–3 d. Food reward is used as a positive reinforcement for establishing an appetitive link and minimizing negative associations<sup>48</sup>.

**▲ CRITICAL STEP** Control the rat's body weight daily. Animals should not lose weight during the habituation procedure.

**? TROUBLESHOOTING**

**17|** Slowly extend the fixation time over a number of days (two or three sessions per day; the number of sessions and the increment in time between sessions should be adapted to the animal behavioral response to fixation). Always provide a food reward at the end of the session for positive reinforcement. From the second or third session onward, upon release from fixation, place the rats in the behavioral arena, where the chocolate reward is provided. Slowly reinstate training to pellet chasing and running until presurgery behavioral performance is reached (as outlined in Steps 1–3).

**18|** When the rat can sit quietly under head-fixation—i.e., without struggling and/or displaying overt behavioral signs of stress—for a minimal period of 15 min (this is typically achieved within 2–3 d), gradually present other individual aspects of the final recording situation; gradually habituate the animal to the lights and noise of the setup equipment (i.e., the stepping sound of the micromanipulator), the head-stage, cables and LED lights while running (a dummy head-stage with LEDs can be used for this purpose). The aim is to gradually habituate the rats to the final recording configuration by trying to mimic it as closely as possible during training<sup>48</sup>. This typically requires an additional 2–3 d.

**▲ CRITICAL STEP** It is important that the steps and manipulations always follow the same order. Gradual habituation to the final recording situation is essential to minimize stress and improve behavioral performance during the recording experiment.

## Juxtacellular recording and labeling ● **TIMING 1–2 d**

**19|** Anesthetize the rat with isoflurane and fix its head firmly by securing the head-post to the holder. Remove the silicone plug from the recording chamber, and perform a small craniotomy under stereomicroscopic guidance. Use a small drill bit (e.g., 0.45 mm in diameter) to drill a circular groove (1.5–2.0 mm in diameter) until the bone at the edges starts to break. Use fine forceps to lift away the circular piece of bone in one piece.

**▲ CRITICAL STEP** This step and Steps 20–22 should be performed under stereomicroscopic guidance.

**▲ CRITICAL STEP** Avoid drilling across the bone, as this might cause excessive bleeding. After removing the bone, the dura should appear intact and no bleeding should occur.

**20|** If you need to remove the dura, apply two drops of bupivacaine to the dura surface, and wait for 3–5 min before washing it thoroughly with Ringer solution. Remove the dura with the help of fine forceps, after making an incision with a hypodermic needle (e.g., 25 gauge). Gently clean the exposed cortex with Ringer solution to remove blood. Craniotomy-induced bleeding usually stops within 2–3 min.

**▲ CRITICAL STEP** Once the dura is removed, keep the brain surface from drying out. Removing the dura is not essential for obtaining juxtacellular recordings, as in young animals the dura can easily be penetrated by the electrode; however, removal of the dura might increase the chances of obtaining stable juxtacellular configurations, as the pipette enters the brain more cleanly.

**21|** If it is necessary to target the exact location and depth, map the location of the target region by recording local field potential and multiunit activity with a low-resistance electrode (e.g., tungsten or glass electrode, 0.5–1 M $\Omega$ ) and a conventional head-stage. Depending on the target brain area—especially for deep brain structures, which are typically more difficult to target solely on the basis of stereotaxic coordinates—this procedure might be necessary for fine-tuning the exact target location and depth.

**22|** Screw the miniaturized micromanipulator on the base and insert a sham pipette. By means of a manual stereotaxic manipulator (**Fig. 2b**), place the pipette tip in the center of the craniotomy. Once the pipette is in the correct position, cement the micromanipulator's base in place by adding a thick layer of dental cement.

**▲ CRITICAL STEP** Tightly secure the micromanipulator's adaptor (see Equipment and **Fig. 2b**) to avoid undesired movements of the pipette tip from its target position during hardening or shrinking of the dental cement.

**23|** Once the dental cement has hardened, release the micromanipulator-base assembly by unscrewing the adaptor piece (**Fig. 2b**). Next, release the micromanipulator by unscrewing the four screws on the base (**Fig. 2**). Only the base remains cemented in place.

**24|** Seal the craniotomy with a layer of silicone sealant and place the animal in the cage for recovery for >4 h.

**▲ CRITICAL STEP** Isoflurane anesthesia is associated with rapid animal recovery. We typically let the animals recover in their home cages for 4–24 h before proceeding to the next step. For times longer than 24 h, apply a drop of antibiotic agent (mitomycin; see Reagent Setup) to the brain surface to minimize the occurrence of tissue regrowth and infections.

**25|** After recovery from isoflurane anesthesia (Step 24), head-fix the animal by following the same procedural sequence used during training (Step 16). Under stereomicroscopic guidance, remove the silicone plug from the craniotomy, evaluate the brain surface and, if necessary, clean the brain exposure.

**▲ CRITICAL STEP** The brain surface should appear clean. If tissue regrowth or signs of infection are observed (typically only for times longer than 24 h after the craniotomy), carefully clean the exposure with Ringer solution and surgery cellulose swabs. Avoid touching the brain surface directly, as this can potentially result in tissue damage.

**26|** Assemble the full recording implant (**Fig. 3**) by first fixing the miniaturized head-stage on the head-post with a thin layer of instant glue (cyanoacrylate). Then fill a pipette (**Fig. 3c**) with pipette solution (see Reagent Setup), and shorten it to an ~2–3-cm total length by cutting the glass with a glass-cutting file. Insert the pipette in the micromanipulator and secure the micromanipulator onto the head-mounted base (**Fig. 3b**).

**27|** Position the electrode wire inside the glass pipette, fix it with a tiny drop of silicone sealant and place the reference wire into the recording chamber. By operating the micromanipulator, slowly advance the pipette under high-magnification stereomicroscopic guidance until it touches the surface of the brain. This position can be taken as a reference for visually estimating the recording depth (see next step).

**28|** Advance the glass pipette into the brain by means of the micromanipulator, until the electrode tip reaches (or is close to) the target area.

**▲ CRITICAL STEP** The linear micromanipulator is not equipped with an absolute depth reader<sup>51</sup>, as this would increase the mass and weight of the device. The desired recording depth, which is obtained from stereotactic atlas<sup>50</sup> and/or mapping experiments (Step 21), is estimated by visually monitoring the distance traveled on the micromanipulator while the animal is head-fixed. In addition, if the target area has characteristic electrophysiological signatures (i.e., ripples or sharp-wave complexes and complex spiking activity in the pyramidal layer of the CA1 region of the hippocampus<sup>43</sup>; nested theta-gamma activity in the medial entorhinal cortex<sup>52</sup>), they can be monitored online in current-clamp configuration while advancing the electrode, and they can be used as an additional readout for localizing the target recording site.

#### ? TROUBLESHOOTING

**29|** Fill the recording chamber with a 3% (wt/vol) agarose solution (see Reagent Setup) by gently applying it with a large-syringe needle (e.g., 20 gauge).

**▲ CRITICAL STEP** Use agarose solution similar to the animal's body temperature.

**30|** If you are going to perform a long recording session (>2 h), consider covering the agarose layer with a thin layer of bone wax or silicone, as this prevents drying of the agarose. Avoid thick layers of bone wax and silicone, as these might compromise the stepping performance of the micromanipulator.

**31|** Release the rat from head-fixation and place it in the behavioral arena.

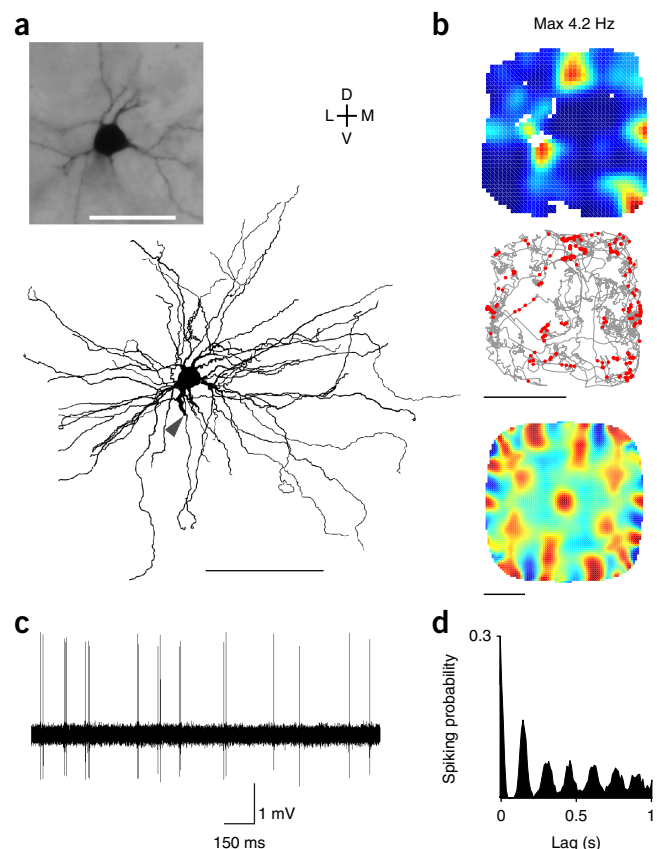


**Figure 4 |** Morphological identification of a grid cell. **(a)** Top: micrograph of a diaminobenzidine-stained 60- $\mu$ m-thick tangential section, showing the soma of a layer 3 neuron of medial entorhinal cortex recorded in a freely moving rat. Scale bar, 50  $\mu$ m. Bottom: tangential projection (top view) of the reconstruction of the basal dendritic field. Gray arrowhead shows the truncated apical dendrite (not shown in this reconstruction). Scale bar, 100  $\mu$ m. D, dorsal; V, ventral; M, medial; L, lateral. **(b)** Top: color-coded rate map (red indicates maximal firing rate, indicated above) showing the spatial activity profile of the recorded neuron (shown in **a**). Middle: spike-trajectory plot showing the animal's trajectory (gray line) and the position at which spikes occurred (red dots). Bottom: 2D spatial autocorrelation of the rate map shown in **b** (top), revealing the hexagonal grid cell periodicity. Scale bar, 50 cm. **(c)** Representative juxtacellular spike-trace recorded during freely moving behavior for the neuron shown in **a**. **(d)** Spike autocorrelogram for the neuron shown in **a**. Note the spiking rhythmicity in the theta-frequency band (4–12 Hz). All animal protocols used in this study were approved by the German guidelines on animal welfare.

## PROTOCOL

**32** | Randomly throw chocolate crumbs in the behavioral arena. While the rat is foraging and actively running, try to establish a juxtacellular recording in the target region by slowly stepping down the micromanipulator (approximately one step every 2–3 s; micromanipulator settings should be adjusted to obtain a 2–4- $\mu$ m step size). Continuously monitor the electrode tip resistance on the oscilloscope by applying small negative current pulses (i.e., –0.5 nA, 200 ms long every 2–3 s). The establishment of a juxtacellular configuration is signaled by an ~2–3 times increase in tip resistance and high signal-to-noise ratio of the spike signals (juxtacellular spike amplitude is typically >2 mV peak to peak; **Fig. 4**).

**▲ CRITICAL STEP** Closely monitor the quality of the juxtacellular recording. This is done by monitoring the unfiltered raw signal and by looking for signs of cellular damage (i.e., negative DC shifts, spikes becoming broader and/or displaying an ‘intracellular-like’ shape). To avoid accidental staining of neurons, quickly discard recordings in which cellular damage occurs. Current pulses for monitoring electrode resistance should have negative polarity in order to avoid spillover of the positively charged Neurobiotin.

**▲ CRITICAL STEP** Head-shaking is a major mechanical disturbance that can lead to the loss of recording. While animals are actively engaged in foraging for food pellets, head-shaking rarely occurs. If needed, the occurrence of head-shaking can be minimized by injecting small volumes (0.1–0.2 ml) of 0.5% (wt/vol) lidocaine solution in the neck region to minimize the discomfort of the head implant.

### ? TROUBLESHOOTING

**33** | If a stable juxtacellular recording is established and is maintained for a sufficient time for the animal to sample the surface of the 1 × 1 m arena, attempt juxtacellular labeling. This is done by modulating the cell’s firing rate (i.e., ‘entrainment’) by injecting typically 5–20 nA square current pulses (50% duty cycle: 200 ms ON, 200 ms OFF). The average duration of the labeling procedure in freely moving animals is 1–3 min. Successful labeling during the entrainment procedure is signaled by broadening of the spikes and small negative DC shifts in the baseline potential. Further details of how to perform juxtacellular labeling can be found in refs. 32–34.

**▲ CRITICAL STEP** Juxtacellular labeling requires close proximity of the pipette tip to the recorded neuron. Attempt the labeling if large amplitude peak-to-peak spike signals (>2 mV) and biphasic action potential shapes are observed, which are indicative of a close somatic or perisomatic location of the recording pipette tip<sup>42</sup>.

**▲ CRITICAL STEP** According to our experience, juxtacellular labeling is typically more difficult in an animal that is actively running compared with a resting animal, possibly because of higher mechanical instability of the juxtacellular configuration during active running. To circumvent this problem and to maximize the success rate of labeling, give a large food pellet to the animal in order to keep it stationary while labeling is attempted. If the juxtacellular recording is accidentally lost during labeling, quickly perfuse the animal (Step 37), as this might improve the chances of recovering the soma and proximal dendrites of the labeled cell.

### ? TROUBLESHOOTING

**34** | Upon successful juxtacellular labeling, slowly retract the electrode.

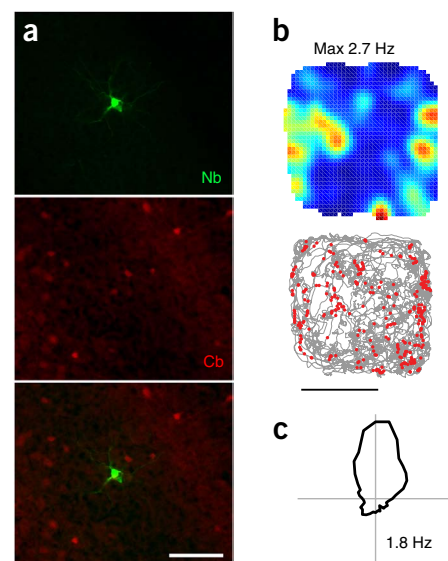
**▲ CRITICAL STEP** Upon electrode retraction, monitor the spiking activity of the recorded cell. Spike shapes and firing rates should return to prelabeling levels. This is to ensure that the transient membrane pores generated upon labeling have resealed and the cell is viable.

**35** | If desired, perform a second penetration for recording and labeling a second neuron in the target region by repeating Steps 27–32. Head-fix the animal and release the micromanipulator from its base and replace the electrode with a new one.

**▲ CRITICAL STEP** Ensure that the two penetrations can be unequivocally assigned by *post hoc* histological analysis. Rotate the micromanipulator within its anchoring base, to ensure that the electrode penetrates in a different location. Note the relative position of the electrode penetration compared with the previous one.

**Figure 5** | Morphological identification of a head-direction cell.

(a) Fluorescence micrograph of a 60- $\mu$ m-thick tangential section stained for Neurobiotin (Nb, green; visualized with streptavidin conjugated to Alexa Fluor 546, 1:1,000) and calbindin (Cb, red; visualized with anti-calbindin antibody, 1:5,000), showing the soma and proximal dendrites of a parasubicular neuron recorded in a freely moving rat. Scale bar, 100  $\mu$ m. (b) Top, color-coded rate map (red indicates maximal firing rate, indicated above) showing the spatial activity profile of the recorded neuron (shown in a). Bottom: spike-trajectory plot showing the animal’s trajectory (gray line) and the position at which spikes occurred (red dots). Scale bar, 50 cm. (c) Firing activity as a function of head direction for the cell shown in a. Note the sharp directional tuning of the neuron. Peak firing rate is indicated. All animal protocols used in this study were approved by the German guidelines on animal welfare.



**36|** Head-fix the animal and remove the head-stage and the micromanipulator from the implant. Seal the craniotomy with silicone and place the animal back in its home cage for a sufficient time to allow complete filling of the recorded cell (typically >2 h). For assessment of dendritic morphology, shorter times (20–30 min) are typically sufficient.

#### ? TROUBLESHOOTING

**37|** Euthanize the animals by overdose injection of anesthetics (e.g., pentobarbital; i.p.). Perfuse the brain transcardially with saline followed by a 4% (wt/vol) paraformaldehyde solution, using standard methods.

**38|** Remove the brain and store it overnight at 4 °C in a 4% (wt/vol) paraformaldehyde solution. Afterward, transfer the brain into PBS solution.

■ **PAUSE POINT** The brain can be stored in the paraformaldehyde solution for up to 2–3 d, and afterward for up to 1–2 weeks in PBS. Longer storage times may decrease the quality of the subsequent stainings.

**39|** Slice the brain with a vibratome (e.g., into 100–150-μm-thick sections) or cryostat (e.g., into 40–60-μm-thick sections) and then process the slices with standard methods, based on the avidin-biotin binding reaction, for visualizing the Neurobiotin-filled cell morphology. Either the diaminobenzidine chromogen, which produces a dark brown reaction product (**Fig. 4a**), or fluorophores (i.e., streptavidin conjugated to Alexa Fluor 546; **Fig. 5a**) can be used for revealing the cell morphology. Further details on Neurobiotin detection methods can be found in refs. 53–55. Reconstruct the 3D neuronal morphology with dedicated computer software (e.g., Neurolucida; **Fig. 4a**).

#### ? TROUBLESHOOTING

Troubleshooting advice can be found in **Table 1**.

**TABLE 1 |** Troubleshooting table.

Step	Problem	Possible reason	Solution
3	After 7 d, the animal behavioral performance is not satisfactory	The animal is stressed	Familiarize the animal more slowly to the experimental procedures Decrease ambient luminance
		Inter-individual differences in behavioral performances	Longer training is required
9,10	The implant does not adhere tightly to the skull	The skull surface is not clean and/or sufficiently dry	Thoroughly clean the skull surface (i.e. no traces of blood and connective tissue) Let the skull dry until the surface appears whitish
		The polymerized adhesive layer is not properly cleaned	Thoroughly clean the polymerized adhesive surface with a cotton swab
		The adhesive does not polymerize properly	Cure the adhesive by UV light for a longer illumination time (up to 1 min) The UV lamp might not work properly. Replace it
16	After 3 d, the animal is not fully habituated to head fixation (i.e., it shows signs of stress)	The habituation time is not sufficient	Habituate the animal for a longer time
		Inter-individual differences in habituation time	Increase the habituation time more slowly in consecutive sessions Reward the animal after each session
28	The electrode does not move upon operation of the micromanipulator	The layer of agarose and bone wax is too thick	Apply less agarose and bone wax. Make sure that the agarose concentration is not >3% (wt/vol)
		Micromotor stepping is impaired	Carefully clean the micromanipulator with 70% (vol/vol) ethanol, following the manufacturer's guidelines Send the micromanipulator to the manufacturer for cleaning and re-calibration

(continued)

**TABLE 1** | Troubleshooting table (continued).

Step	Problem	Possible reason	Solution
28	Electrode dechlorides quickly	A fluid contact occurs between the aluminum implant components and the Ringer solution in the recording chamber	Isolate the aluminum components and avoid direct fluid contact If the problem persists, consider replacing the aluminum with stainless steel (which is, however, heavier)
32	Cellular or membrane damage consistently occurs after establishment of the juxtacellular configuration (i.e., recordings become partially intracellular)	Suboptimal pipette-tip shape Pipette resistance is too high (i.e., too-small pipette tips)	Replace the electrode
		The osmolarity of the internal solution is not within the target range (310–315 mOsm/liter) or the Neurobiotin concentration is too high (>3% wt/vol)	Make a new batch of pipette solution and check the osmolarity
	Juxtacellular recordings cannot be obtained (no ‘hits’ are observed, i.e., increases in electrode tip resistance)	The electrode is broken, or the tip is too large (i.e., electrode resistance is <1–2 MΩ) The electrode is clogged (i.e., tip resistance is >20–30 MΩ in the brain)	Replace the electrode
		Excessive brain tissue movements and pulsations	Make a smaller craniotomy Agarose solution: make sure the concentration is not lower than 3% (wt/vol) and that the agarose solution has hardened before proceeding to the recordings
33	Juxtacellular recordings are consistently lost within 1–2 min	The tip shape is suboptimal (i.e., irregular or too small)	Replace the electrode Add thin layer of silicone (Kwik-Cast) on top of the agarose. This provides additional mechanical stability to the preparation
		Insufficient mechanical stability	Ensure that the motor and the pipette are tightly screwed
		The craniotomy is too large	Make a smaller craniotomy
		The agarose gel is not sufficiently thick	Make new agarose solution. Make sure the concentration is not lower than 3% (wt/vol) and that the agarose solution has hardened before proceeding to the recordings
		Electrode wire is too long and stiff, i.e., motion-related movements of the wire are translated to the electrode	Use thinner and shorter electrode wires
		The electrode is too long	Cut the electrode to the maximal size of ~2–3 cm
	Cells are consistently lost during labeling	Animal running destabilizes the labeling	Attempt labeling when the animal is resting
		Labeling current intensity increases too quickly	Slowly increase the amplitude of the injected current; quickly decrease it once the dielectric membrane resistance is broken, i.e., upon sudden increase in spiking activity

(continued)

**TABLE 1** | Troubleshooting table (continued).

Step	Problem	Possible reason	Solution
	Exceptionally high currents (>30 nA) are needed for entraining the cell	Pipette tip is too large	Pull a new electrode, reduce the pipette tip size
		Pipette tip is too far from the recorded cell	Step closer to the recorded cell; spikes should be of large amplitude and of biphasic shape
33, 36	The cell is not recovered	Entrainment of the cell is insufficient	Label or entrain the cell for longer times and/or higher injection currents
		Concentration of Neurobiotin is too low	Make a new batch of pipette solution
		The cell dies after labeling	After labeling, carefully monitor the cell's spiking activity upon slowly retracting the electrode. The cell membrane should re-seal and spiking activity should go back to the pre-labeling baseline

## ● TIMING

Steps 1–3, animal behavioral training: 7–10 d

Steps 4–15, implantation and animal recovery: 3–6 d

Steps 16–18, habituation to head fixation and training: 4–6 d

Steps 19–39, juxtacellular recording and labeling: 1–2 d

## ANTICIPATED RESULTS

With the current protocol, the spiking activity of single, morphologically identified neurons can be monitored while animals are freely behaving. This approach has proved instrumental in elucidating structure-function relationships in the spatial memory circuits<sup>8,56</sup>. As an example, here we show the anatomical identification of spatially modulated neurons—a grid cell<sup>57</sup> (**Fig. 4**) and a head-direction cell<sup>58,59</sup> (**Fig. 5**)—which are thought to contribute to an internal representation of external space<sup>60,61</sup>. The grid cell was recorded in layer 3 of medial entorhinal cortex<sup>57</sup>, which is known to contain morphologically distinct cell types differing in intrinsic properties, projection patterns and connectivity<sup>62,63</sup>. The recorded neuron was identified and classified as a large pyramidal neuron (**Fig. 4a**), located in the upper layer 3 (layer 2/3 border). **Figure 4a** shows a reconstruction of the basal dendrites of the recorded neuron. Note the large spread of the basal dendritic field within layer 3, extending for up to 322  $\mu\text{m}$  and 371  $\mu\text{m}$  along the dorso-ventral and medio-lateral axis, respectively. During exploration, firing activity of this neuron occurred at multiple spatial locations showing hexagonal symmetry (grid-score (ref. 64) = 0.53; **Fig. 4b**), a defining feature of grid cell activity<sup>57</sup>, and it was modulated at theta frequency (4–10 Hz; **Fig. 4c,d**). Notably, grid cells can, at present, be unequivocally identified only in unrestrained animals, exploring large open-field environments, where the grid periodicity can be revealed<sup>57</sup>. This protocol thus provides a unique approach for studying the cellular basis of the ‘cognitive’ grid representation. The head-direction cell was recorded in the parasubiculum<sup>41,65</sup>. **Figure 5a** shows a raw fluorescent micrograph of a 60- $\mu\text{m}$ -thick tangential section, costained for calbindin immunoreactivity (red). The soma of the recorded neuron (green) and the few proximal dendrites contained within this thin section can be observed (**Fig. 5a**). This cell did not show any clear spatial firing pattern (**Fig. 5b**), but spiking activity was sharply tuned to the animal's heading direction (**Fig. 5c**), consistent with the known properties of ‘pure’ head-direction coding neurons<sup>58,64</sup>. In these two examples, juxtacellular recordings (i.e., biphasic spikes with peak-to-peak amplitude >2 mV; **Fig. 4c**) were maintained for 16 min (**Fig. 4**) and 14 min (**Fig. 5**) before the labeling protocol was initiated. Within these times, the animals sampled 63% (**Fig. 4b**) and 77% (**Fig. 5b**) of the available surface of a large 1  $\times$  1 m open-field arena, which provided sufficient spatial coverage for assessing the functional properties of the recorded neurons.

In summary, the methodology described here represents a step forward toward filling the long-standing gap between extracellular recordings and single-cell identification methods. It provides the means for exploring the functional implications of single-cell heterogeneity, and it is an addition to the portfolio of currently available methods aimed at resolving the cellular and circuit basis of animal behavior.

**ACKNOWLEDGMENTS** We thank A. Stern and M. Kunert (Berlin, Germany) and K. Vollmer (Tübingen, Germany) for excellent fine mechanical support, and U. Schneeweiß and J. Steger for excellent technical support. We are particularly grateful to R. Naumann and S. Ray for histological processing of the cells shown in **Figures 4** and **5**, U. Schneeweiß for reconstructing the neuron shown in **Figure 4a** and C. Mende for contributions to figures. We thank G. Doron for comments on earlier versions of the manuscript. This work was supported by Neurocore, the Bernstein Center for Computational Neuroscience (BMBF) and Humboldt University, an EU Biotact-grant and a Neuro-behavior European Research Council grant.

**AUTHOR CONTRIBUTIONS** A.B. and Q.T. performed experiments in the establishment of the protocol. A.B. and M.B. supervised the experiments. A.B. drafted the manuscript. Q.T., M.B. and A.B. contributed to, and have approved, the final version of the manuscript.

**COMPETING FINANCIAL INTERESTS** The authors declare no competing financial interests.

Reprints and permissions information is available online at <http://www.nature.com/reprints/index.html>.

- Klausberger, T. & Somogyi, P. Neuronal diversity and temporal dynamics: the unity of hippocampal circuit operations. *Science* **321**, 53–57 (2008).
- Krook-Magnuson, E., Varga, C., Lee, S.H. & Soltesz, I. New dimensions of interneuronal specialization unmasked by principal cell heterogeneity. *Trends Neurosci.* **35**, 175–184 (2012).
- Klausberger, T. *et al.* Brain-state- and cell-type-specific firing of hippocampal interneurons *in vivo*. *Nature* **421**, 844–848 (2003).
- Ascoli, G.A. *et al.* Petilla terminology: nomenclature of features of GABAergic interneurons of the cerebral cortex. *Nat. Rev. Neurosci.* **9**, 557–568 (2008).
- Lee, W.C.A. & Reid, R.C. Specificity and randomness: structure-function relationships in neural circuits. *Curr. Opin. Neurobiol.* **21**, 801–807 (2011).
- Harris, K.D. & Mrsic-Flogel, T.D. Cortical connectivity and sensory coding. *Nature* **503**, 51–8 (2013).
- Varga, C., Lee, S.Y. & Soltesz, I. Target-selective GABAergic control of entorhinal cortex output. *Nat. Neurosci.* **13**, 822–824 (2010).
- Ray, S. *et al.* Grid-layout and theta-modulation of layer 2 pyramidal neurons in medial entorhinal cortex. *Science* **343**, 891–896 (2014).
- Kerr, J.N.D. *et al.* Spatial organization of neuronal population responses in layer 2/3 of rat barrel cortex. *J. Neurosci.* **27**, 13316–13328 (2007).
- de Kock, C.P.J. & Sakmann, B. Spiking in primary somatosensory cortex during natural whisking in awake head-restrained rats is cell-type specific. *Proc. Natl. Acad. Sci. USA* **106**, 16446–16450 (2009).
- Dong, H.-W., Swanson, L.W., Chen, L., Fanselow, M.S. & Toga, A.W. Genomic-anatomic evidence for distinct functional domains in hippocampal field CA1. *Proc. Natl. Acad. Sci. USA* **106**, 11794–11799 (2009).
- Thompson, C.L. *et al.* Genomic anatomy of the hippocampus. *Neuron* **60**, 1010–1021 (2008).
- Kamme, F. *et al.* Single-cell microarray analysis in hippocampus CA1: demonstration and validation of cellular heterogeneity. *J. Neurosci.* **23**, 3607–3615 (2003).
- Oberlaender, M. *et al.* Three-dimensional axon morphologies of individual layer 5 neurons indicate cell type-specific intracortical pathways for whisker motion and touch. *Proc. Natl. Acad. Sci. USA* **108**, 4188–4193 (2011).
- Fenno, L., Yizhar, O. & Deisseroth, K. The development and application of optogenetics. *Annu. Rev. Neurosci.* **34**, 389–412 (2011).
- Zhang, F. *et al.* Optogenetic interrogation of neural circuits: technology for probing mammalian brain structures. *Nat. Protoc.* **5**, 439–456 (2010).
- Deisseroth, K. & Schnitzer, M.J. Engineering approaches to illuminating brain structure and dynamics. *Neuron* **80**, 568–577 (2013).
- Wang, J. *et al.* Integrated device for combined optical neuromodulation and electrical recording for chronic *in vivo* applications. *J. Neural Eng.* **9**, 016001 (2012).
- Anikeeva, P. *et al.* Optetrode: a multichannel readout for optogenetic control in freely moving mice. *Nat. Neurosci.* **15**, 163–170 (2011).
- Prakash, R. *et al.* Two-photon optogenetic toolbox for fast inhibition, excitation and bistable modulation. *Nat. Methods* **9**, 1171–1179 (2012).
- Zhang, F. *et al.* Multimodal fast optical interrogation of neural circuitry. *Nature* **446**, 633–639 (2007).
- Aravanis, A.M. *et al.* An optical neural interface: *in vivo* control of rodent motor cortex with integrated fiber-optic and optogenetic technology. *J. Neural Eng.* **4**, S143–S156 (2007).
- Lee, J.H. *et al.* Global and local fMRI signals driven by neurons defined optogenetically by type and wiring. *Nature* **465**, 788–792 (2010).
- Cardin, J.A. *et al.* Targeted optogenetic stimulation and recording of neurons *in vivo* using cell-type-specific expression of channelrhodopsin-2. *Nat. Protoc.* **5**, 247–254 (2010).
- Chung, K. *et al.* Structural and molecular interrogation of intact biological systems. *Nature* **497**, 332–337 (2013).
- Kepecs, A. & Fishell, G. Interneuron cell types are fit to function. *Nature* **505**, 318–326 (2014).
- Battaglia, D., Karagiannis, A., Gallopin, T., Gutch, H.W. & Cauli, B. Beyond the frontiers of neuronal types. *Front. Neural Circuits* **7**, 13 (2013).
- Denk, W., Briggman, K.L. & Helmstaedter, M. Structural neurobiology: missing link to a mechanistic understanding of neural computation. *Nat. Rev. Neurosci.* **13**, 351–358 (2012).
- Lang, S., Derksen, V.J., Sakmann, B. & Oberlaender, M. Simulation of signal flow in 3D reconstructions of an anatomically realistic neural network in rat vibrissa cortex. *Neural Netw.* **24**, 998–1011 (2011).
- Potjans, T.C. & Diesmann, M. The cell-type specific cortical microcircuit: relating structure and activity in a full-scale spiking network model. *Cereb. Cortex* **24**, 785–806 (2014).
- Brown, S.P. & Hestrin, S. Cell-type identity: a key to unlocking the function of neocortical circuits. *Curr. Opin. Neurobiol.* **19**, 415–421 (2009).
- Pinault, D. Golgi-like labeling of a single neuron recorded extracellularly. *Neurosci. Lett.* **170**, 255–260 (1994).
- Deschênes, M., Bourassa, J. & Pinault, D. Corticothalamic projections from layer V cells in rat are collaterals of long-range corticofugal axons. *Brain Res.* **664**, 215–219 (1994).
- Pinault, D. A novel single-cell staining procedure performed *in vivo* under electrophysiological control: morpho-functional features of juxtacellularly labeled thalamic cells and other central neurons with biocytin or Neurobiotin. *J. Neurosci. Methods* **65**, 113–136 (1996).
- Pinault, D. The juxtacellular recording-labeling technique. In *Electrophysiol. Rec. Tech. Neuromethods* (eds. Vertes, R.P. & Stackman, R.W. Jr.) **54**, 41–75 (Humana Press, 2011).
- Pinault, D., Bourassa, J. & Deschênes, M. The axonal arborization of single thalamic reticular neurons in the somatosensory thalamus of the rat. *Eur. J. Neurosci.* **7**, 31–40 (1995).
- Houweling, A. & Brecht, M. Behavioral report of single neurons stimulation in somatosensory cortex. *Nature* **451**, 65–69 (2008).
- Milevskiy, B. & Morales, M. Duration of inhibition of ventral tegmental area dopamine neurons encodes a level of conditioned fear. *J. Neurosci.* **31**, 7471–7476 (2011).
- Boucetta, S., Cisse, Y., Mainville, L., Morales, M. & Jones, B.E. Discharge profiles across the sleep-waking cycle of identified cholinergic, GABAergic, and glutamatergic neurons in the pontomesencephalic tegmentum of the rat. *J. Neurosci.* **34**, 4708–4727 (2014).
- Pinault, D. & Deschênes, M. Projection and innervation patterns of individual thalamic reticular axons in the thalamus of the adult rat: a three-dimensional, graphic, and morphometric analysis. *J. Comp. Neurol.* **391**, 180–203 (1998).
- Burgalossi, A. *et al.* Microcircuits of functionally identified neurons in the rat medial entorhinal cortex. *Neuron* **70**, 773–786 (2011).
- Herfst, L. *et al.* Friction-based stabilization of juxtacellular recordings in freely moving rats. *J. Neurophysiol.* **108**, 697–707 (2012).
- Lee, A.K., Epsztein, J. & Brecht, M. Head-anchored whole-cell recordings in freely moving rats. *Nat. Protoc.* **4**, 385–392 (2009).
- Judkewitz, B., Rizzi, M., Kitamura, K. & Häusser, M. Targeted single-cell electroporation of mammalian neurons *in vivo*. *Nat. Protoc.* **4**, 862–869 (2009).
- Veenman, C.L., Reiner, A. & Honig, M.G. Biotinylated dextran amine as an anterograde tracer for single- and double-labeling studies. *J. Neurosci. Methods* **41**, 239–254 (1992).
- Furuta, T., Kaneko, T. & Deschênes, M. Septal neurons in barrel cortex derive their receptive field input from the lemniscal pathway. *J. Neurosci.* **29**, 4089–4095 (2009).
- Domnisoru, C., Kinkhabwala, A.A. & Tank, D.W. Membrane potential dynamics of grid cells. *Nature* **495**, 199–204 (2013).
- Schwarz, C. *et al.* The head-fixed behaving rat—procedures and pitfalls. *Somatosens. Mot. Res.* **27**, 131–148 (2010).

49. Muller, R.U., Kubie, J.L. & Ranck, J.B. Spatial firing patterns of hippocampal complex-spike cells in a fixed environment. *J. Neurosci.* **7**, 1935–1950 (1987).
50. Paxinos, G. & Watson, C. *The Rat Brain in Stereotaxic Coordinates* (Elsevier Science, 2006).
51. Lee, A.K., Manns, I.D., Sakmann, B. & Brecht, M. Whole-cell recordings in freely moving rats. *Neuron* **51**, 399–407 (2006).
52. Mizuseki, K., Sirota, A., Pastalkova, E. & Buzsáki, G. Theta oscillations provide temporal windows for local circuit computation in the entorhinal-hippocampal loop. *Neuron* **64**, 267–280 (2009).
53. Horikawa, K. & Armstrong, W.E. A versatile means of intracellular labeling: injection of biocytin and its detection with avidin conjugates. *J. Neurosci. Methods* **25**, 1–11 (1988).
54. Huang, Q., Zhou, D. & DiFiglia, M. Neurobiotin, a useful neuroanatomical tracer for *in vivo* anterograde, retrograde and transneuronal tract-tracing and for *in vitro* labeling of neurons. *J. Neurosci. Methods* **41**, 31–43 (1992).
55. Marx, M., Günter, R.H., Hucko, W., Radnikow, G. & Feldmeyer, D. Improved biocytin labeling and neuronal 3D reconstruction. *Nat. Protoc.* **7**, 394–407 (2012).
56. Brecht, M. *et al.* An isomorphic mapping hypothesis of the grid representation. *Philos. Trans. R. Soc. Lond. B. Biol. Sci.* **369**, 20120521 (2014).
57. Hafting, T., Fyhn, M., Molden, S., Moser, M.-B. & Moser, E.I. Microstructure of a spatial map in the entorhinal cortex. *Nature* **436**, 801–806 (2005).
58. Taube, J.S., Muller, R.U. & Ranck, J.B. Head-direction cells recorded from the postsubiculum in freely moving rats. I. Description and quantitative analysis. *J. Neurosci.* **10**, 420–435 (1990).
59. Taube, J.S. The head direction signal: origins and sensory-motor integration. *Annu. Rev. Neurosci.* **30**, 181–207 (2007).
60. Moser, E.I., Kropff, E. & Moser, M.-B. Place cells, grid cells, and the brain's spatial representation system. *Annu. Rev. Neurosci.* **31**, 69–89 (2008).
61. Moser, E.I. & Moser, M.-B. Grid cells and neural coding in high-end cortices. *Neuron* **80**, 765–774 (2013).
62. Canto, C.B. & Witter, M.P. Cellular properties of principal neurons in the rat entorhinal cortex. II. The medial entorhinal cortex. *Hippocampus* **22**, 1277–1299 (2012).
63. Burgalossi, A. & Brecht, M. Cellular, columnar and modular organization of spatial representations in medial entorhinal cortex. *Curr. Opin. Neurobiol.* **24**, 47–54 (2014).
64. Sargolini, F. *et al.* Conjunctive representation of position, direction, and velocity in entorhinal cortex. *Science* **312**, 758–762 (2006).
65. Boccara, C.N. *et al.* Grid cells in pre- and parasubiculum. *Nat. Neurosci.* **13**, 987–994 (2010).